Table II. Fluorescence Lifetimes and Rate Constants of DCA-1,5-DMN Exciplex in the Vapor Phase ($\tau = \lambda_1^{-1}$)[a]

excitation wavelength, nm			
385		420	
T, K	τ, ns	T, K	τ, ns
DCA (1×10^{-6} M) + 1,5-DMN (2×10^{-2} M)			
496	40.8	505	40.0
516	37.0	514	37.4
527	34.5	529	34.4
541	33.6	544	31.7

	rate constant		
	k_3', M^{-1} s^{-1}	k_4, s^{-1}	$(k_5 + k_6)$, s^{-1}
DCA + 1,5-DMN	9.1×10^{10}	1.2×10^7	1.5×10^7

[a] Errors of fluorescence lifetimes are approximately ±1. Rate constants were determined at 513 K.

$= 9.1 \times 10^{10}$ M^{-1} s^{-1}. The fluorescence intensity ratio of DCA in the absence (I_0) and presence (I) of the electron donor is expressed by the following equation:[12]

$$I_0/I - 1 = k_3'[D](k_5 + k_6)/(k_4 + k_5 + k_6)(k_1 + k_2)$$

Plots of I_0/I vs. [D] are shown in Figure 7. Combining the slope of these plots with k_3' and the lifetimes of the exciplex and the DCA fluorescence, the dissociation rate constant of the exciplex (k_4) was obtained to be 1.2×10^7 s^{-1} as summarized in Table II. It is noteworthy that the dissociation rate constant of the exciplex is significantly large in comparison with $k_5 + k_6$ as summarized in Table II, which implies that the dissociation process to DCA and 1,5-DMN is unusually important in the deactivation of the exciplex.

The fluorescence lifetimes of the exciplex of DCA-1,5-DMN vapor in the absence of the buffer gas are independent of the excitation wavelength, while those of the collision-free exciplex in DCAN are remarkably dependent, as mentioned above. In the intermolecular exciplex formation in the vapor phase, the concentration of 1,5-DMN (10^{-2}-10^{-3} M) as the electron donor corresponds to the gas pressure of ~50 torr and the rate of the exciplex formation ($k_3'[D]$) is approximately 10^8-10^9 s^{-1}. The collisional relaxation rate by 1,5-DMN itself is estimated to be 5×10^8 s^{-1} from the hard-sphere collision model, which is comparable to the rate of the exciplex formation. These arguments of the reaction rates suggest that 1,5-DMN act not only as an electron donor but also as a relaxer of the upper vibrational state of the S_1 state of DCA. Therefore, the exciplex fluorescence lifetimes of DCA-1,5-DMN vapor even in the absence of the buffer gas cannot depend on the excitation wavelength.

Prochorow et al.[5] suggested that the radiationless decay of the gas-phase TCNB-*p*-xylene exciplex was very sensitive to temperature variation and that the low-frequency intermolecular deactivation played an important role in the radiationless deactivation of the exciplex. The exciplex fluorescence in the DCA-1,5-DMN vapor decreases in intensity in comparison with that of DCA fluorescence with increasing temperature, while the intramolecular exciplex in DCAN vapor shows less significant temperature dependence. The dissociation process of the intermolecular exciplex in the DCA-1,5-DMN vapor is important in the deactivation of the exciplex, as mentioned above. In the intramolecular exciplex, however, the dissociation rate constant is known to be much lower than the association rate constant, and also much lower than the dissociation rate constant in the corresponding intermolecular system. Therefore, the facts in the DCAN vapor suggest that the dissociation of the DCAN exciplex to DCA and naphthyl moieties does not seem to be the most important decay channel of the radiationless deactivation of the exciplex.

Acknowledgment. This work was partially supported by the Grant-in-Aid for Scientific Research (No. 410404 and 447115) from in Ministry of Education, Science and Culture of Japan.

A Theoretical Investigation of the Structure and Rotational Barriers of Peroxyformimidic Acid. The Mechanism of Stereomutation at the Carbon-Nitrogen Double Bond

Timothy J. Lang, Gregory J. Wolber, and Robert D. Bach*

Contribution from the Department of Chemistry, Wayne State University, Detroit, Michigan 48202. *Received August 18, 1980*

Abstract: The relative energies of the eight planar structures of peroxyformimidic acid have been studied employing ab initio MO calculations. The minimum energy conformer has the *Z* configuration about the C=N bond and an anti configuration about the O-O bond. The C-O and O-O rotational barriers were calculated to be 6.61 and 3.75 kcal/mol, respectively, employing a 6-31G basis set. The inversion barrier at nitrogen was calculated to be 15.9 kcal/mol (6-31G) and compared to a calculated topomerization barrier in methylenimine of 25.2 kcal/mol. The relevance of these calculations to the epoxidation of alkenes with peroxyformimidic acid is discussed.

Introduction

A significant role is played by 1,2-epoxides (oxiranes) in both biological and industrial chemical processes. Synthetic intermediates containing this highly reactive[1] functional group are typically prepared from alkenes on an industrial scale by the use of organic peroxides and metal catalysts,[2] whereas in the laboratory use is made of a variety of peroxy acids.[3] The latter method appears to require the intermediacy of a weakly basic heteroatom that is intramolecularly hydrogen bonded to a hydroperoxide.

Despite the extensive use of such reagents, the ground-state structures of this important class of organic peroxides have not

(1) Berti, G. *Top. Stereochem.* **1973**, *7*, 93.
(2) Sharpless, K. B.; Verhoeven, T. R. *Aldrichimica Acta* **1979**, *12*, 63.

(3) (a) House, H. O. "Modern Synthetic Reactions", 2nd ed.; W. A. Benjamin: Menlo Park, CA, 1972; p 292. (b) Harrison, I. T.; Harrison, S. "Compendium of Organic Synthetic Methods", Wiley-Interscience: New York, 1971; p 325. *Ibid.*; 1974; Vol. II; p 134. (c) Swern, D. *Org. React.* **1953**, *7*, 378.

0002-7863/81/1503-3275$01.25/0

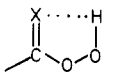

X = O, N

yet been fully elucidated. The inherent instability of the peracid moiety has limited detailed structural investigations. However, X-ray crystal analysis of *o*-nitroperbenzoic acid[4a] and peroxypelargonic acid[4b] has established the OCOO portion of these molecules to be essentially planar. There have also been several theoretical investigations of the structures of simple peracids using semiempirical[5] and ab initio[6] methods of calculation. Recently, we reported a theoretical study of the structure and rotational barriers of peroxyformic acid (**1**).[7] Our ab initio calculations suggested that the molecule has a minimum energy in its planar anti conformation **1**. Using the Gaussian 70 series of programs,[8] we calculated a surprisingly low oxygen–oxygen torsional barrier for the interconversion (eq 1) of **1** to **1a** (syn conformer). The

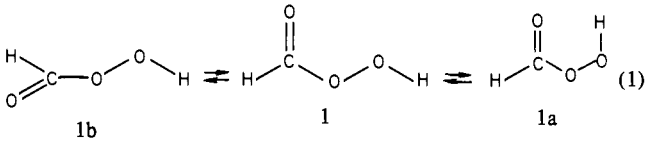

1b 1 1a (1)

O–O rotational barriers ranged from 1.55 kcal/mol with an STO-3G basis set to 1.04 kcal/mol with an extended 5-31G basis set. These barriers are lower than the calculated O–O barrier for peroxyacetic acid (3–4 kcal/mol).[5c] This may possibly be attributed to our adherence to full geometry optimization at each calculated point on the rotational surface. The calculated bond angles and distances were in good accord with the reported X-ray data.[4] The C–O rotational barrier (**1** → **1b**) was calculated to be 7.68 kcal/mol which is also well below the 13.2- and 12.9-kcal/mol C–O barriers that have been calculated for the ester, methyl formate.[9]

We have previously reported both theoretical[10a] and experimental studies[10b] on the epoxidation of alkenes. More recently we have developed a procedure for the large-scale (3 mol) epoxidation of cyclooctene using a peroycarboximidic acid.[10c] Such reagents are readily generated in situ from the addition of hydrogen peroxide to the nitrile functional group (eq 2). The

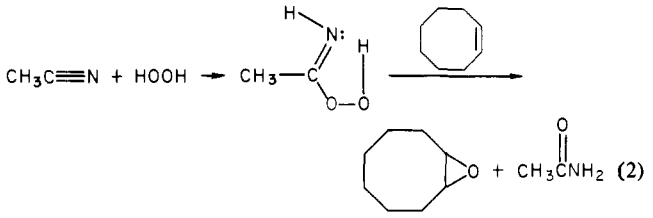

(2)

principal advantage of this epoxidation procedure is the utilization of H_2O_2 as the oxidant. The method was initially developed by Payne[11] and has since been extended by Rebek[12] and in our own laboratory.[10b,c] In the absence of an alkene these reagents, which may be construed as imino derivatives of peroxy acids, are reduced in alkaline media by a second mole of H_2O_2. The kinetics of alkaline decomposition of peroxybenzamidic acid was first studied by Wiberg[13] who showed the products to be benzamide and oxygen (eq 3). These highly reactive perimidic acids have to our knowledge not yet been isolated.

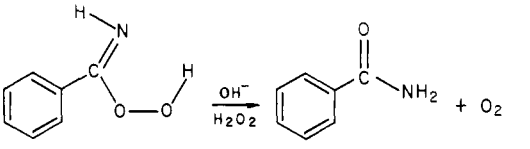

(3)

The dual objective of the present study is to provide the first structural data, albeit theoretical, for peroxyimidic acids and to compare these data with our previous study on peroxyformic acid.[7] We choose peroxyformimidic acid as our model substrate since this is the simplist compound in this class.

Method of Calculation

All calculations were performed on an Amdahl Model 470V/6 computer. The ab initio molecular orbital calculations were carried out with the Gaussian 70 program with standard MO theory.[8] The geometries of the eight planar structures **2–9** were first minimized with a minimal

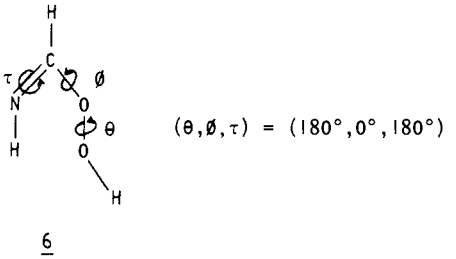

6

$(\theta,\phi,\tau) = (180°,0°,180°)$

Figure 1. Bond angles for peroxyformimidic acid (**6**).

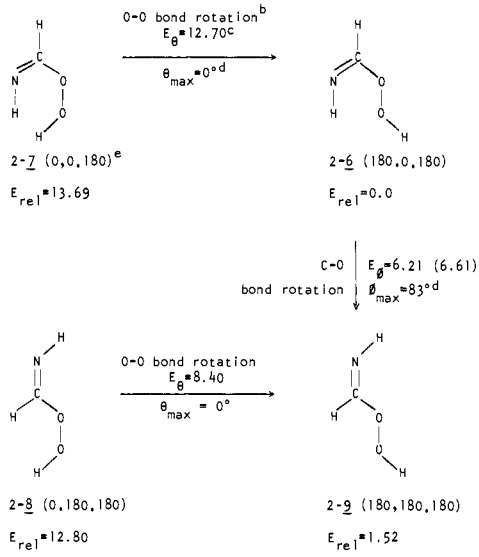

a) Relative energies are given in kcal/mol calculated with a 6-31G basis set. The total energy of 2-6 = -243.54572 a.u. A conversion factor of 627.514 kcal/a.u. was used.

b) Barrier to O-O bond rotation (E_θ) and C-O bond rotation (E_ϕ) are given in kcal/mol with an STO-3G basis set.

c) Rotational barrier for 180° O-O bond rotation, kcal/mol.

d) Maximum on the reaction surface in deg. for bond rotation.

e) Value in deg. for O-O bond angle θ, C-O bond angle φ and C=N bond angle τ.

f) Rotational barrier in parenthesis employed a 6-31G basis set.

Figure 2. Relative energies of planar conformers of (*Z*)-peroxyformimidic acid.[a]

(4) (a) Sax, M.; Beurskens, P.; Chu, S. *Acta Crystallogr.* **1965**, *18*, 252. (b) Belitskus, D.; Jeffery, G. A. *Ibid.* **1965**, *18*, 458.
(5) (a) Yonezawa, T.; Kato, H.; Yamamoto, O. *Bull. Chem. Soc. Jpn.* **1967**, *40*, 307. (b) Azman, A.; Borstnik, B.; Plesnican, B. *J. Org. Chem.* **1969**, *34*, 971. (c) Hjelmeland, L. M.; Loew, G. H. *Chem. Phys. Lett.* **1975**, *32*, 309; *Tetrahedron* **1977**, *33*, 1029.
(6) (a) Plesnicar, B.; Taserski, M.; Azman, A. *J. Am. Chem. Soc.* **1978**, *100*, 743. (b) Azman, A.; Koller, J.; Plesnicar, B. *Ibid.* **1979**, *101*, 1107.
(7) Bach, R. D.; Willis, C. L.; Lang, T. J. *Tetrahedron* **1979**, *35*, 1239.
(8) Hehre, W. J.; Stewart, R. F.; Pople, J. A. *J. Chem. Phys.* **1969**, *51*, 2657.
(9) Wennerstrom, H.; Forsen, S.; Roos, B. *J. Phys. Chem.* **1972**, *76*, 2430; John, I. G.; Radom, L. *J. Mol. Struct.* **1977**, *36*, 133.
(10) (a) Bach, R. D.; Willis, C. L.; Domagala, J. M. "Applications of MO Theory in Organic Chemistry", Csizmadia, I. G., Ed.; Elsevier: New York, 1977; Vol. II; p 221. (b) Bach, R. D.; Klein, M. W.; Ryntz, R. A.; Holubka, J. W. *J. Org. Chem.* **1979**, *44*, 2569. (c) Bach, R. D.; Knight, J. W. *Org. Syn.*, in press.
(11) Payne, G. B.; Deming, P. H.; Williams, P. H. *J. Org. Chem.* **1961**, *26*, 659. Payne, G. B. *Tetrahedron* **1962**, *18*, 763.
(12) Rebek, J.; Wolf, S.; Mossman, A. *J. Org. Chem.* **1978**, *43*, 180.
(13) Wiberg, K. B. *J. Am. Chem. Soc.* **1953**, *75*, 3961.

Table I. Calculated Geometry of the Planar Conformers of Peroxyformimidic Acid[a]

(θ, ϕ, τ)[b]	struct	O–O[c]	O–C	C=N	O–H	C–H	N–H	O–O–H	O–O–C	O–C–H	O–C=N	C=N–H
(0, 0, 0)	**2**	1.401	1.393	1.273	1.005	1.095	1.039	102.23	110.71	111.06	119.97	110.69
		1.449	1.359	1.251	0.970	1.073	0.999	104.01	113.23	109.77	120.83	118.85
(180, 0, 0)	3	1.404	1.401	1.272	1.002	1.096	1.044	98.79	107.79	108.78	123.18	108.08
		1.449	1.366	1.245	0.957	1.076	1.002	99.42	112.67	106.74	124.99	116.09
(180, 180, 0)	4	1.404	1.406	1.273	0.999	1.097	1.044	99.35	105.66	113.85	117.93	108.12
		1.455	1.379	1.245	0.955	1.073	1.002	101.00	107.08	112.50	118.36	116.40
(0, 180, 0)	5	1.401	1.406	1.272	1.002	1.099	1.044	105.45	112.76	115.13	117.89	108.33
		1.450	1.380	1.243	0.960	1.079	1.002	108.69	114.66	114.17	118.68	117.04
(180, 0, 180)	6	1.403	1.409	1.270	0.998	1.093	1.046	99.26	106.95	109.48	128.55	108.49
		1.451	1.389	1.243	0.956	1.070	1.004	100.87	109.87	107.88	128.38	117.96
(0, 0, 180)	7	1.399	1.405	1.272	1.001	1.095	1.045	105.88	116.11	107.45	132.85	112.15
		1.445	1.382	1.247	0.958	1.069	1.002	108.81	118.63	106.81	131.17	123.05
(0, 180, 180)	8	1.401	1.406	1.271	1.002	1.096	1.047	105.19	113.42	116.30	122.67	108.26
		1.448	1.386	1.244	0.960	1.073	1.006	108.00	115.63	115.50	122.63	117.72
(180, 180, 180)	9	1.403	1.407	1.272	1.000	1.094	1.048	99.41	106.42	115.09	122.70	108.24
		1.453	1.387	1.246	0.956	1.068	1.006	101.13	108.07	113.77	122.40	117.74

[a] All geometries were exhaustively optimized using an STO-3G basis set (top values) and an extended 631-G basis set (lower values) with the molecule in a planar conformation. [b] See Figure 1 for the specific angles given. [c] Bond lengths and angles are in angstroms and degrees, respectively.

Table II. Fourier Expansion Coefficients for O–O and C–O Rotation

	V_1	V_2	V_3	V_4	V_5	V_6	max, deg	barrier, kcal/mol
				6-31G				
2 → **3**	2.908	1.540	0.6735	0.3472	0.1331	0.0481	147	3.75
				STO-3G				
2 → **3**	0.8214	0.0272	0.1234	0.3660	0.1910	0.0764	120	1.20
5 → **4**	−9.114	−3.380	−0.6819	0.0586	0.0446	0.0167	0	9.75
7 → **6**	−10.148	−5.491	−0.9873	−0.0021	0.0355	0.0126	0	12.7
8 → **9**	−7.776	−3.228	−0.6610	0.0397	0.0281	0.0146	0	8.4
				C–O Rotation				
STO-3G	−0.0287	5.846	0.8158	0.0690	−0.0215	−0.0230	83	6.21

STO-3G basis set and then with a extended 6-31G basis set using the above 3G geometric parameters as initial input. The results of optimization of bond angles to within ±0.1° and bond distances to 0.01 Å are given in Table I.

The O–O and C–O rotational barriers were obtained from a plot of seven fully optimized structures generated by altering the requisite dihedral angles θ (C–O–O–H) and ϕ (N=C–O–O) by 30° increments between the limits of 0 and 180° (Figure 1). All variables were minimized at each point with the exception of ϕ and τ which were maintained at either 0° (**2**–**4**) or 180° (**5**–**8**) to keep the remainder of the molecule planar. The inversion angle at nitrogen, η, was also minimized at each point on the rotational surface. An STO-3G basis set was used throughout with the exception of the O–O rotational barrier for the conversion of **2** to **3** where an extended 6-31G basis set was also employed with full geometry optimization. In addition, a single geometry was optimized (6-31G) for the C–O torsional barrier at ϕ = 90°.

The barriers to O–O and C–O rotational maxima were obtained by fitting the data obtained at 30° intervals to a truncated Fourier expansion as described previously[7] for peroxyformic acid (eq 4). For the O–O

$$E_\theta - E_{(\theta\ \mathrm{min})} = \sum_{K=1}^{6} V_K \frac{1 - \cos K\theta}{2} - V_0 \qquad (4)$$

barrier the terms $E_\theta - E_{(\theta\ \mathrm{min})}$ represent the calculated total energy (kcal/mol) for the conformer with dihedral angle θ (θ = 0° in *E*-**2** and 180° in *E*-**3**) relative to the energy minimum having an angle θ_{min}. The parameter V_0 is the energy of the minimum energy conformer *E*-**2** relative to the (180°, 0°, 0°) conformer **3**, and V_K's are the Fourier expansion coefficients which can be determined from the resulting linear system of equations. We determined the values in Table II (kcal/mol) for the coefficients representing the hindering potential for the interconversion of the planar structures given in Figures 2 and 3. For the particular barrier of **2** → **3**, a 6-31G basis set was also employed. All other fully calculated torsional barriers were determined with an STO-3G basis set.

The barrier to torsion about the C=N bond and the barrier to inversion at nitrogen was calculated with an STO-3G basis set with full geometry optimization at 30° intervals. The maximum on the inversion barrier for conversion of **3** to **6**, η = 180°, was calculated by 6-31G with full geometry optimization. The combined rotation–inversion of **2** → **7** and **3** → **6** given in Figures 8 and 9 utilized a STO-3G basis set. The C=N torsional angle τ was varied at 45° intervals at the following fixed

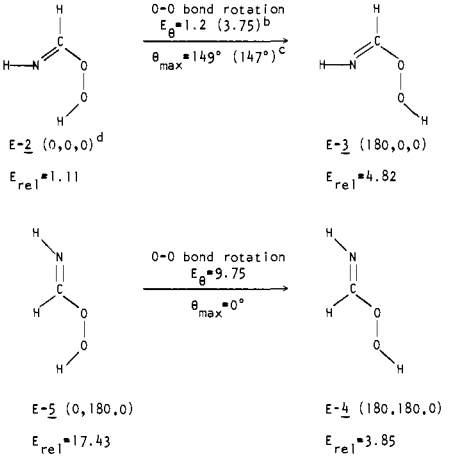

a) Relative energies are given in kcal/mol calculated with a 6-31G basis set.

b) Barrier to O-O bond rotation in parenthesis employed a 6-31G basis set (kcal/mol).

c) Maximum in deg. on reaction surface for O-O bond rotation (6-31G).

d) See Fig. 2, footnote e.

Figure 3. Relative energies of planar conformers of (*E*)-peroxyformimidic acid.[a]

angles of inversion at nitrogen: η = 90, 120, 150, and 175°. The barrier heights for C=N torsion at those values of η are given relative to the ground-state energies of *E*-**2** and *Z*-**6**. All other pertinent variables were minimized at each value of η.

The geometry of our model compound, methylenimine, was fully optimized by 6-31G using a 4-31G[14a] geometry for an initial geometry. Its topomerization barrier was based upon the difference in the ground-state

(14) (a) Wolf, S.; Schlegel, H. B.; Whangbo, M. H. *Can. J. Chem.* **1976**, *54*, 795. (b) Lathan, W. A.; Curtiss, L. A.; Hehre, W. J.; Lisle, J. B. *Prog. Phys. Org. Chem.* **1975**, *11*, 175.

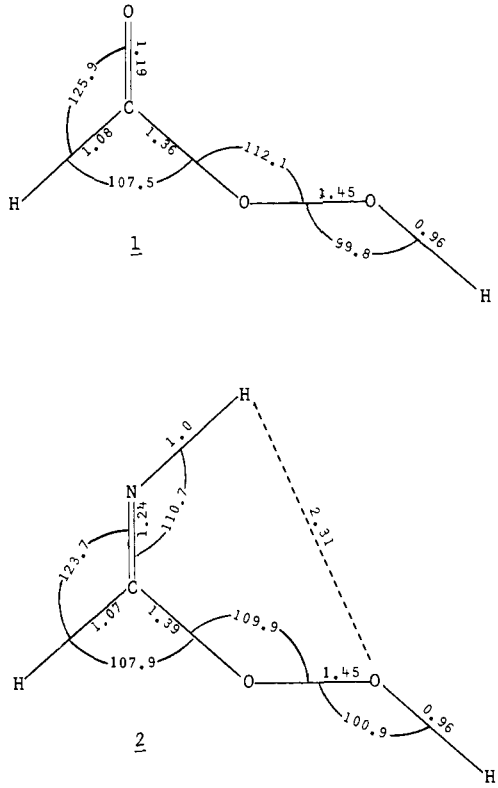

Figure 4. Comparison of the 6-31G optimized geometries of peroxyformic acid and peroxyformimidic acid.

energy **12** and **12a** (η = 180°). The geometry of HCN was optimized at a 6-31G level while H_2O_2 was calculated by 6-31G using a 4-31G optimized geometry[14b] assuming an antiplanar conformation.

Results and Discussion

The synthetic utility of peroxyimidic acids as oxidizing agents and their intrinsic instability prompted our theoretical investigation of the structure and dynamics of this peroxy functional group. The imino moiety renders this class of compounds more complex to study than peroxy acids because of the potential existence of both *Z* and *E* stereoisomers of the imino double bond. In addition, we must consider the s-cis and s-trans configurations about the partial double-bond character of the imino carbon–oxygen bond and the syn and anti periplanar conformers of the oxygen–oxygen single bond. We shall use the above nomenclature as a matter of convenience in the ensuing discussion. Because of the complexity of this problem we first directed our attention toward

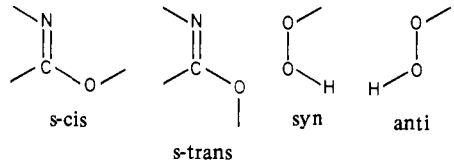

geometry optimization of the eight possible planar structures of the simplest peroxyimidic acid, peroxyformimidic acid.

Planar Peroxyformimidic Acid. Inspection of the calculated relative energies (6-31G) for the planar structures **2–9** given in Figures 2 and 3 indicate that the *Z* isomer **6** exhibits an energy minimum in its s-cis geometry with an antiperiplanar arrangement about the peroxide bond. It is of interest to note that the anti conformer in peroxyformic acid (**1**) was also found to be an energy minimum.[7] A comparison of the calculated geometries of **1** and **6** (Figure 4) show them to be remarkably similar in nature with identical O–O bond lengths.

Rotation (180°) about the C–O bond in **6** affords the planar s-trans conformer **9** that is only 1.52 kcal/mol higher in total energy. However, O–O bond rotation to produce the syn periplanar structures **7** and **8** results in substantial increases in energy (13.69 and 12.80 kcal/mol, respectively). Since the *Z* isomers

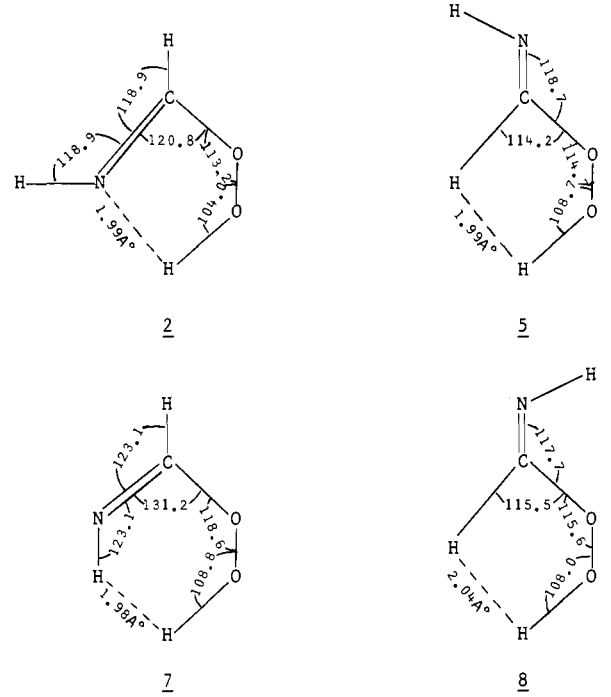

Figure 5. Bond angles for planar peroxyformimidic acid (6-31G).

are several kcal/mol *lower* in energy than the corresponding *E* conformers, we attribute the energy increases in **5**, **7**, and **8** to serious hydrogen–hydrogen nonbonding interactions. These repulsive interactions are manifested in an increase in internal bond angles that is particularly evident in **7** where the O—C=N bond angle is 131.2° (Figure 5). The internuclear H···H bond distances in the isomers **5**, **7**, and **8** are ~2.0 Å. In contrast, the N···H internuclear bond distance of 1.99 Å in *E*-**2** results in a *decrease* in total energy as a result of hydrogen bonding. This conformer is only 1.11 kcal/mol above the minimum energy conformer **6** which has the *Z* imino configuration. With peroxyimidic acids derived from addition of H_2O_2 to acetonitrile or benzonitrile, conformers corresponding to **5** and **8** should be essentially unpopulated because of nonbonding steric interactions.

Isomerization of (*Z*)- and (*E*)-Peroxyformimidic Acid. We next examined the possible mechanisms for interconversion of the *Z* and *E* stereoisomers. This question is relevant to the use of peroxyimidic acids as epoxidizing agents since the peroxy hydrogen transfer to the nitrogen in the transition state for alkene epoxidation can best be achieved with planar conformer *E*-**2** (vide infra). We calculated the formation of *E*-**2** from HCN and H_2O_2 to be exothermic by −19.0 (STO-3G) and −3.54 (6-31G) kcal/mol (eq 5). However, our experimental data suggests that the for-

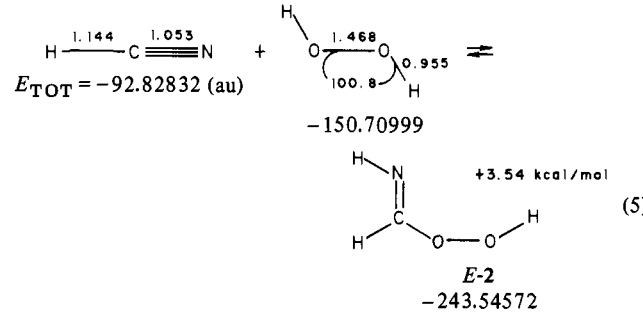

(5)

mation constant for *E*-**2** is not very high in solution. Alternatively, equilibration of the *Z*–*E* isomers may be attained by torsion about the C=N double bond, by inversion at imino-nitrogen, or by an intermediate mechanism that has both torsional and inversional components.[15]

(15) Kalinowski, H.-O.; Kessler, H. *Top. Stereochem.* **1977**, *7*, 295.

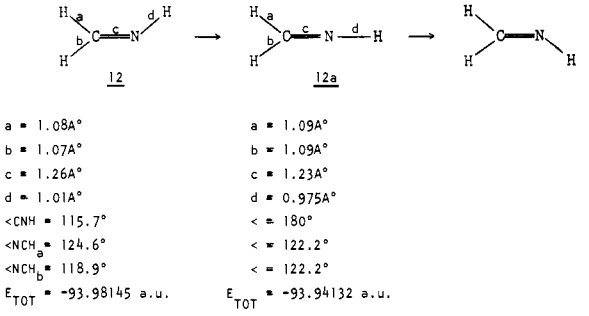

Figure 6. Topomerization of methylenimine.

Although it is generally thought that *Z*–*E* isomerization of imines is largely an inversional process,[15] Raban has presented arguments that some torsional character may be involved.[16] Heteroatoms (N or O) attached to the imino carbon caused small increases in the inversion barrier but dramatic decreases in the calculated torsional barriers. When two nitrogens were present the rotational barrier had been lowered by more than 30 kcal/mol and was calculated to be lower than the barrier to nitrogen inversion. On this basis it was suggested[16] that the effect of heteroatoms in lowering experimental barriers to stereomutation in imines could be attributed to a torsional component in the overall barrier. Resonance structure **10a** provides a rationale for the increased torsional participation and the attendant decreases in the barrier of isomerization of **10** to **11** as a consequence of the

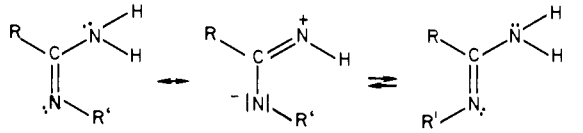

10 **10a** **11**

reduction in C=N double-bond character. A second facet of the present study was to try to distinguish between the two pathways for nitrogen inversion.

The inversion process, or lateral-shift mechanism, was calculated for the interconversion of *E*-**2** to *Z*-**7** and *E*-**3** to *Z*-**6** since these two examples involve both syn and anti configurations of the peroxide bond (eq 6 and 7). As anticipated, the maxima for pure

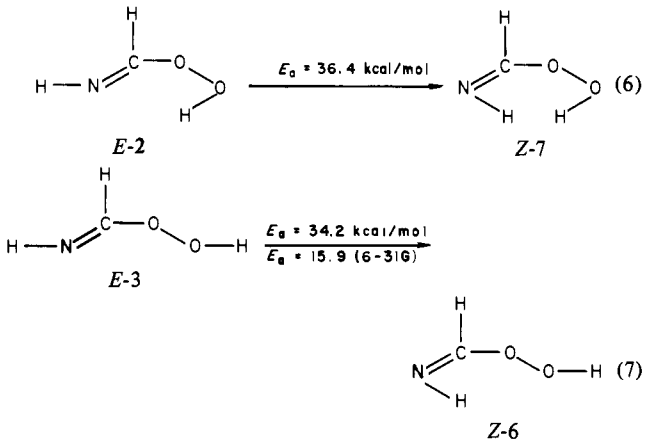

inversion were observed when essentially a linear arrangement of C=N—H (η = 180°) was attained with all atoms lying in a common plane. Inversion barriers of 36.4 and 34.2 kcal/mol (STO-3G) were observed with the latter barrier being reduced to 15.9 kcal/mol when an extended 6-31G basis set was employed.

In an effort to determine the effect of the lone pair of the peroxy moiety on the inversion barrier in **2** and **3**, we calculated the corresponding barrier in the parent compound, methylenimine

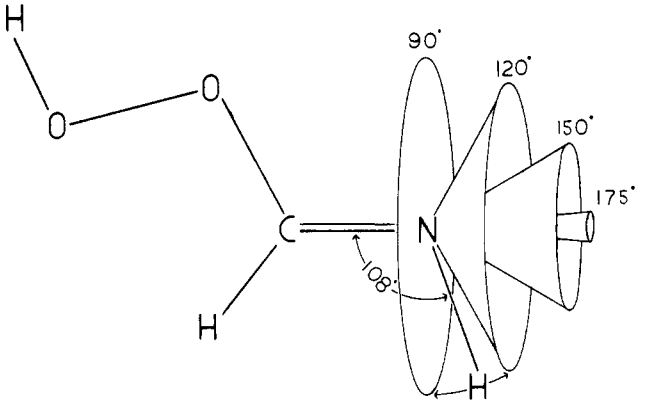

Figure 7. Combined torsional and inversion pathway for *Z*–*E* isomerization in **3** at selected values of η = 90, 120, 150, and 175°.

Table III. Total Energies for Optimized Structures of Peroxyformimidic Acid at Selected Values of τ and η (STO-3G) given in au

	η			
τ	90°	120°	150°	175°
0°	-240.45403[a]	-240.46898	-240.43899	-240.41628
	-240.45532[b]	-240.46526	-240.43363	-240.41689
45°	-240.42273	-240.44022	-240.42621	-240.41552
	-240.41919	-240.43334	-240.42153	-240.41657
90°	-240.37447	-240.39318	-240.40804	-240.41421
	-240.36048	-240.38796	-240.40861	-240.41637
135°	-240.40566	-240.42455	-240.41567	-240.41365
	-240.41996	-240.43648	-240.42374	-240.41696
180°	-240.43344	-240.45263	-240.42600	-240.41365
	-240.45850	-240.4700	-240.43684	-240.41744

[a] Upper values are for the rotational barrier for the conversion of **2** to **7** (Figure 8). [b] Lower values are for the torsional barriers in Figure 9 (3 → 6).

(**12**), with the same basis sets. Topomerization of **12** proceeded with a calculated activation energy of 41.0 kcal/mol (STO-3G) and 25.2 kcal/mol (6-31G). The 6-31G minimized geometries are given in Figure 6. In an earlier ab initio study on methylenimine, Lehn[17] reported barriers to nitrogen inversion and to rotation about the C=N bond of 26–28 and 56 kcal/mol, respectively, when an extended basis set was employed. These studies clearly indicate that the inversion mechanism has a markedly lower energy of activation than the rotational pathway. Furthermore, nitrogen inversion in **3** is 9.3 kcal/mol lower than that calculated for **12**. Thus, the heteroatom effect on imine inversion in the present ab initio study is working in the opposite sense to that reported with semiempirical calculations.[16] While the inversion barrier experiences a modest decrease with a heteroatom substituent, we note that the rotational barrier is decreased from 56 kcal/mol[17] for methylenimine (**12**) to approximately 47.5 kcal/mol for peroxyformimidic acid, in good accord with earlier predictions.[16]

We next designed a theoretical probe to measure the amount of torsional contribution to imine isomerization in our model peroxyimidic acid. If the lowest barrier itinerary is indeed a combination of inversion and rotation, then we would anticipate that a small torsional component would provide a lower barrier than pure inversion. We initially varied the C=N rotation angle τ from 0 to 180° at fixed values of nitrogen inversion angle η = 90, 120, 150, and 175°. These intermediate pathways are depicted schematically in Figure 7 for the isomerization of (*E*)-peroxyimidic acid (**3**). Examination of the total energies for the fully optimized

(16) (a) Raban, M. *Chem. Commun.* **1970**, 1415. (b) Raban, M.; Carlson, E. *J. Am. Chem. Soc.* **1971**, *93*, 685.

(17) Lehn, J. M.; Munsch, B.; Millie, P. H. *Theor. Chim. Acta* **1970**, *16*, 351. For other theoretical studies on this molecule see ref 18.

(18) (a) DeFrees, D. J.; Hehre, W. J. *J. Phys. Chem.* **1978**, *82*, 391. (b) Epiotis, N. D.; Yates, R. L.; Larson, J. R.; Kirmaier, C. R.; Bernardi, F. *J. Am. Chem. Soc.* **1977**, *99*, 8379, and references therein. (c) Osamura, Y.; Kitaura, K.; Nishimoto, K.; Yamabe, S. *Chem. Phys. Lett.* **1979**, *63*, 406.

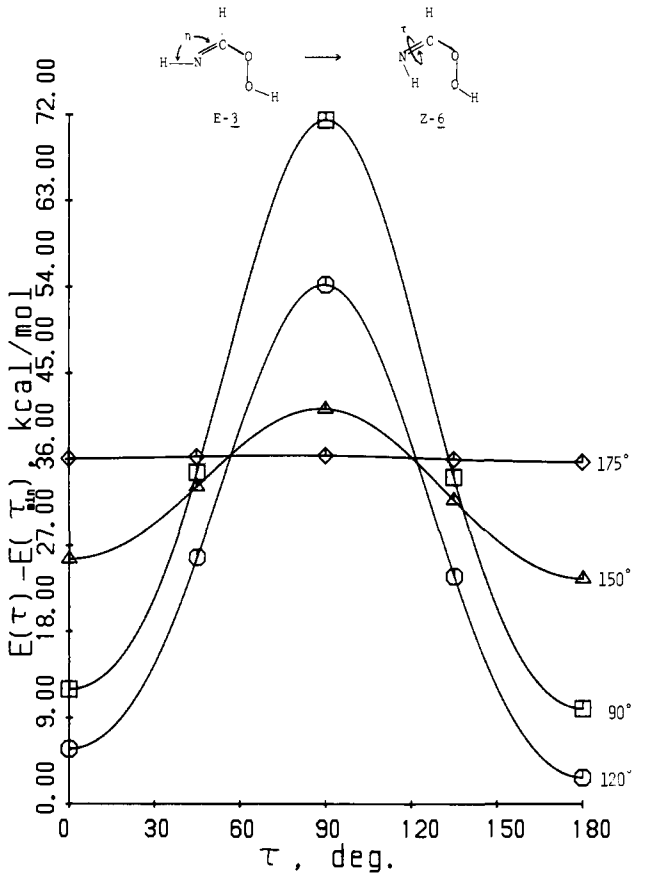

Figure 8. Rotational barrier for torsion about the C=N bond (τ = 0 to 180°) at fixed angles (η = 90, 120, 150, 175°) of nitrogen inversion (STO-3G).

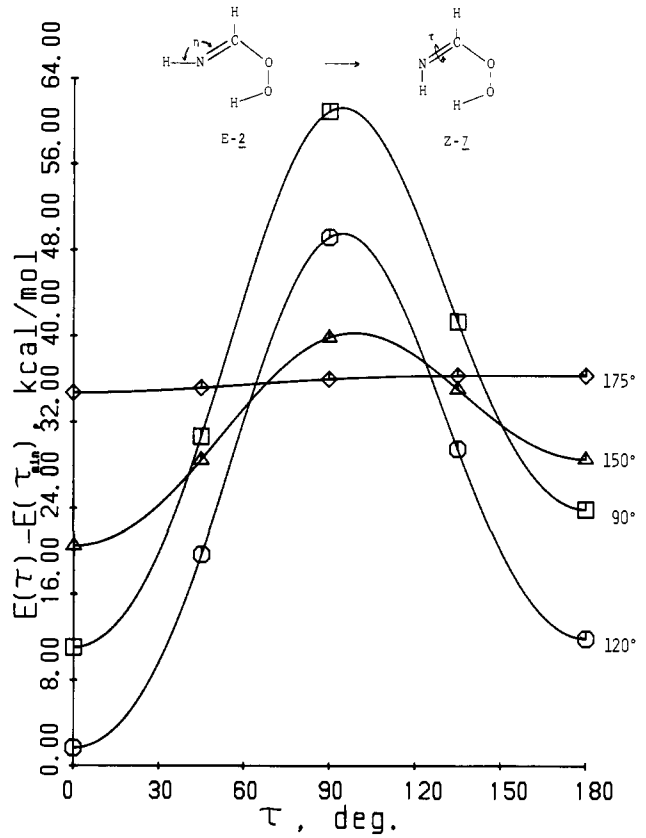

Figure 9. Rotational barrier for torsion about the C=N bond (τ = 0 to 180°) at fixed angles (η = 90, 120, 150, 175°) of nitrogen inversion (STO-3G).

structures at the selected values of τ and η given in Table III, and the rotational plots given in Figures 8 and 9, clearly indicate that, within the constraints of the above experiments, the isomerization of both **2** and **3** involves nearly pure inversion. Only the torsional barrier with η = 175° was lower in energy (0.3–0.7 kcal/mol, STO-3G) than pure inversion. Because the barrier difference between the pure inversion path (η = 180°) and the nearly planar 175° combined inversion–rotation was so small, we examined several values of η around the transition state (τ = 90°) by 6-31G. When η = 175 and 165° the total energy *increased* by 0.1 and 1.1 kcal/mol, respectively, relative to the planar transition state for pure inversion. *These data preclude any detectable torsional component to the Z–E isomerization pathway when the substituent on nitrogen is a hydrogen.*

Carbon–Oxygen Bond Rotation. The magnitude of the C–O rotational barrier in peroxyformimidic acid will determine the relative populations of planar structures. The C–O torsional barrier is largely due to π-bonding between carbon and oxygen as represented by the charged canonical structure **6a**. The C–O

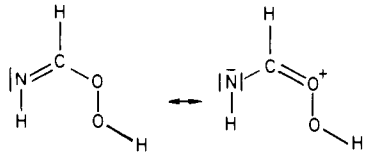

6 6a

barriers in *tert*-butyl formate (8.8 kcal/mol),[19a] formic anhydride (4.4 kcal/mol),[19b] and methyl formate (13.1 kcal/mol)[19c] have been measured experimentally. Theoretical values for the latter ester have also been reported.[9] We recently reported the C–O torsional barrier in peroxyformic acid (**1**) to be 7.68 kcal/mol (STO-3G), in good agreement with the NMR barrier for *tert*-butyl formate. We now report the C–O barrier in *Z*-**6**, which affords *Z*-**9** upon 180° bond rotation (angle ϕ) to exhibit a maximum at ϕ = 83° with calculated barriers of 6.2 kcal/mol (STO-3G) and 6.6 kcal/mol (6-31G). With barriers of this magnitude we can suggest that peroxyformimidic acid will be essentially planar in the gas and most likely in a nonpolar solvent as well. Furthermore, the relative energies given in Figures 2 and 3 suggest that planar conformers **2**, **6**, and **9** should be most highly populated. It therefore remains to examine the oxygen–oxygen torsional barrier to estimate the preferred ground-state structure of peroxyformimidic acid.

Oxygen–Oxygen Bond Rotation. The four O–O rotations that serve to interchange the syn and anti planar conformers were calculated with an STO-3G basis set. As anticipated the relative ground-state energies (Figures 2 and 3) dominated the barriers to O–O torsion with one exception. The 180° O–O bond rotation of *E*-**2** afforded *E*-**3** with a calculated barrier of 1.2 kcal/mol. This relatively low barrier, which is quite comparable to the O–O barrier in peroxyformic acid (**1**), prompted us to compare the barrier to internal rotation in H_2O_2 using the same (STO-3G) basis set. Pople has reported a dihedral angle of 125° for H_2O_2 at the energy minimum.[20] We found the 0 and 180° rotamers of H_2O_2 to be 10.4 and 0.2 kcal above that minimum. Hence, this method of calculation actually exaggerated the magnitude of the experimentally observed (7 kcal) syn barrier in H_2O_2.[22] Because of the significance of this equilibrium to the overall

(19) (a) Drakenberg, T.; Forsen, S. *J. Phys. Chem.* **1972**, *76*, 3582. (b) Noe, E. A.; Raban, M. *Chem. Commun.* **1974**, 479. (c) Miyazawa, T. *Bull. Chem. Soc. Jpn.* **1961**, *34*, 691.

(20) The experimental values for H_2O_2 are r_{OH} = 0.950 Å, r_{OO} = 1.475 Å, HOO angle 94.8° and θ = 111.5°, while the calculated values[21] are 1.001 Å, 1.396 Å, 101.1°, and 125 ± 2°, respectively, with a total energy of −93,365.5 kcal/mol.

(21) Newton, M. D.; Lathan, N. A.; Hehre, W. J.; Pople, J. A. *J. Chem. Phys.* **1970**, *52*, 4064.

(22) Redington, R. L.; Olson, W. B.; Cross, P. C. *J. Chem. Phys.* **1962**, *36*, 1311; Hunt, R. H.; Leacock, R. A.; Peters, C. W.; Hecht, K. T. *Ibid.* **1965**, *42*, 1931.

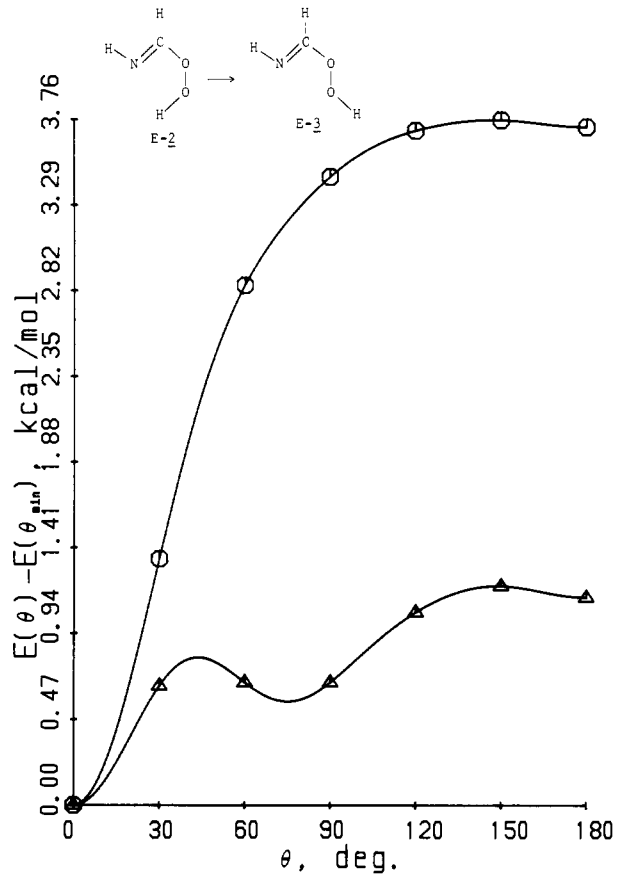

Figure 10. Torsion about the oxygen–oxygen bond in peroxyformimidic acid STO-3G (△) and 6-31G (□).

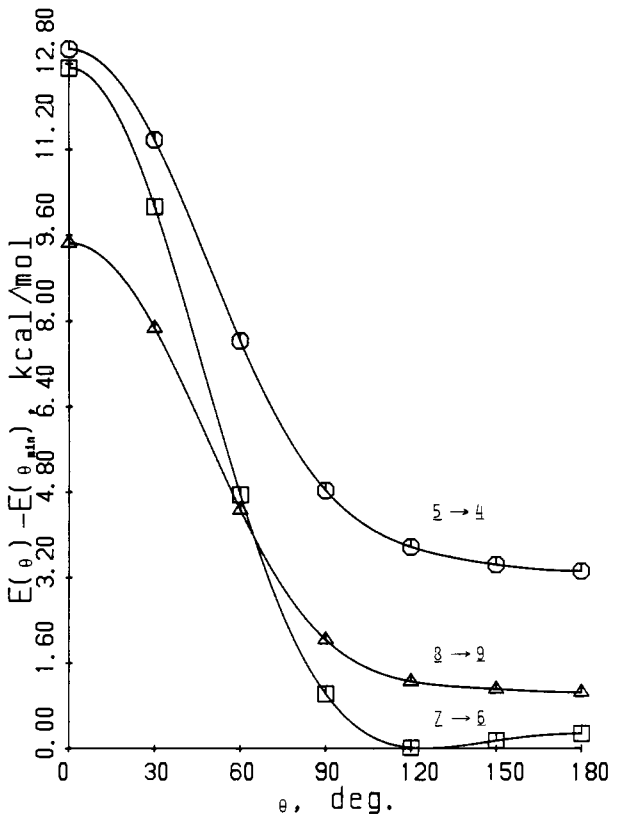

Figure 11. Torsional barriers for the oxygen–oxygen bond in peroxyformimidic acid (STO-3G).

epoxidation mechanism, we also calculated the *E*-**2** to *E*-**3** O–O barrier with an extended 6-31G basis set and observed an increase in the barrier to 3.75 kcal/mol (Figure 10). The remaining O–O

Table IV

dihedral angles, deg			E_{TOT}, au (STO-3G)	E_{rel}, kcal/mol	E_{TOT}, au (6-31G)	E_{rel}, kcal/mol
θ	ϕ	τ				
			2 → 3			
0	0	0	−240.47162	0.00	−243.54395	0.00
30	0	0	−240.47058	0.65	−243.54180	1.35
60	0	0	−240.47055	0.67	−243.53941	2.85
90	0	0	−240.47055	0.67	−243.53846	3.45
120	0	0	−240.46994	1.05	−243.53806	3.70
150	0	0	−240.46971	1.20	−243.53797	3.75
180	0	0	−240.46981	1.14	−243.53803	3.71
			5 → 4			
0	180	0	−240.45402	9.75		
30	180	0	−240.45672	8.06		
60	180	0	−240.46269	4.31		
90	180	0	−240.46715	1.51		
120	180	0	−240.46883	0.46		
150	180	0	−240.46936	0.13		
180	180	0	−240.46956	0.00		
			7 → 6			
0	0	180	−240.45458	12.71		
30	0	180	−240.45871	10.12		
60	0	180	−240.46728	4.74		
90	0	180	−240.47322	1.01		
120	0	180	−240.47483	0.00		
150	0	180	−240.47461	0.14		
180	0	180	−240.47440	0.27		
			8 → 9			
0	180	180	−240.45978	8.41		
30	180	180	−240.46231	6.82		
60	180	180	−240.46773	3.42		
90	180	180	−240.47160	0.99		
120	180	180	−240.47285	0.21		
150	180	180	−240.47308	0.06		
180	180	180	−240.47318	0.00		

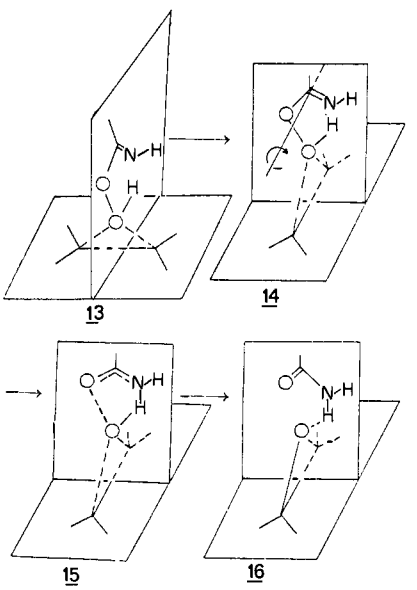

Figure 12. Reaction pathway for alkene epoxidation.

rotational curves are given in Figure 11 and reflect the large difference in ground-state energies that arise principally from the aforementioned H- - -H nonbonding interactions. The relative energies for these rotational surfaces are given in Table IV.

Mechanism of the Epoxidation Reaction. On the basis of the above theoretical analysis we wish to draw the following conclusions concerning the mechanism of alkene epoxidation with peroxyimidic acids. The *Z* conformers may be excluded from any epoxidation mechanism requiring a 1,4-hydrogen transfer unless the rearrangement is accompanied by inversion of configuration at nitrogen. Based upon the calculated inversion barrier this would

result in a prohibitively high activation energy. Rotamer *E*-**5** may be excluded because of its high ground-state energy. Of the remaining *E* conformers only *E*-**2** has the desired proximity of the basic nitrogen lone pair to the incipient hydrogen that is to be transferred in the transition state, **15**, for epoxidation. Significantly, this conformer will be highly populated as a result of its inherent stability. We therefore suggest that the syn *E* conformer **2** is the effective oxidizing agent in oxirane formation with an alkene.

By analogy to our previous theoretical study on the mechanism of epoxidation of alkenes with peroxyformic acid (**1**),[10a] we invoke a backside displacement by the carbon–carbon π-bond (HOMO) on the empty σ^* orbital of the peroxide bond with the orientation depicted in **13**. The transition state **15** may be achieved by O–O bond cleavage, and simultaneous conversion of the initial carbon–oxygen single bond into the carbonyl group of the product formamide by rotation about an axis through the formimide carbon atom and perpendicular to the imine plane (see **14**). The process is accompanied by a concomitant 1,4-hydrogen shift (**16**) which is necessary to effect a net bonding interaction between the terminal oxygen and the alkene carbon.

In conclusion, the overall epoxidation reaction can best be achieved by interaction of *E*-**2** with an alkene as suggested in Figure 12. The above conformational study indicates that this desired conformer is readily attainable and represents a large fraction of the equilibrium mixture of peroxyformimidic acid rotamers.

Acknowledgment. We gratefully acknowledge support from the National Institutes of Health (2 R01 ES00761-08A1) and the National Science Foundation (CHE-80-06520). The authors also wish to thank Professor Morton Raban for helpful discussions concerning the mechanism of imine isomerization and Dr. Frank Westervelt for generous amounts of computer time.

Principal Components of the Cadmium-113 Shielding Tensors in Cadmium Sulfate Hydrates: Nuclear Magnetic Resonance Study of Cadmium Coordinated with Oxygen

P. DuBois Murphy and B. C. Gerstein*

Contribution from Ames Laboratory,† Department of Energy, and Iowa State University, Ames, Iowa 50011. *Received August 22, 1980*

Abstract: A study is reported of the principal components of the ^{113}Cd NMR shielding tensors in the salts $3CdSO_4 \cdot 8H_2O$ and $CdSO_4 \cdot H_2O$. A discussion of the sensitivity of the principal components of the ^{113}Cd shielding tensors to coordination of the cadmium with nearest-neighbor oxygens is presented. An apparent anomaly between the observed shielding anisotropies and the proposed Cd–O bonding distances for $3CdSO_4 \cdot 8H_2O$ has prompted a refinement of the original crystal structure proposed by Lipson. The refined Cd–O bonding distances are found to be more uniform than those originally reported, in agreement with information inferred from the observed ^{113}Cd NMR shielding anisotropies.

Introduction

Solid-state, high-resolution NMR[1] provides a simple, yet powerful means for structural studies. Cheung et al.[2] have recently noted that ^{113}Cd shieldings are particularly sensitive to coordination with oxygen. Their studies showed a ^{113}Cd shielding dispersion of almost 300 ppm among the hydrated salts $2CdCl_2 \cdot 5H_2O$, $Cd(OH)_2 \cdot H_2O$, $3CdSO_4 \cdot 8H_2O$, $Cd(OAc) \cdot 2H_2O$, and $Cd(NO_3)_2 \cdot 4H_2O$. They also noted the two magnetically inequivalent ^{113}Cd species in the salt $3CdSO_4 \cdot 8H_2O$. Although Cheung et al. were not able to resolve the principal components of the two shielding tensors, they did observe that the apparent anisotropies of these tensors were the smallest of those studied.[2]

The purpose of the present work is to measure the principal components of the ^{113}Cd shielding tensors in the hydrated cadmium salts $3CdSO_4 \cdot 8H_2O$ and $CdSO_4 \cdot H_2O$. A comparison is made between the shielding parameters of Cd(II) in $3CdSO_4 \cdot 8H_2O$ and those[2] of the Cd(II) in $Cd(NO_3) \cdot 4H_2O$ for which the crystal structure is believed accurate. In particular, we note an incompatibility between the NMR data and Lipson's proposed crystal structure for $3CdSO_4 \cdot 8H_2O$: the observed ^{113}Cd shielding anisotropies do not appear consistent with the large variation in Cd–O bonding distances proposed by Lipson.[3] This observation has prompted a refinement, discussed below, of the crystal structure of $3CdSO_4 \cdot 8H_2O$.

Experimental Section

Instrumentation. ^{113}Cd-^1H cross polarization (CP) NMR measurements were performed at frequencies of 12.42 and 56.02 MHz for ^{113}Cd and ^1H in our 1.3-T laboratory field. The spectrometer was designed in our laboratory and is described in detail elsewhere.[2] The CP contact time was t_{CP} = 4 ms, rotating-frame H_1 fields were 8 and 36 G, and the time between scans was 3 s for $3CdSO_4 \cdot 8H_2O$ and 9 s for $CdSO_4 \cdot H_2O$. Both magic-angle-spinning (MAS)[1] and off magic-angle-spinning (OMAS)[4,5] experiments were performed with rotor speeds of 2.5 kHz. Static measurements resulted from 8000/15 000 signal averages; MAS and OMAS, 500/800. The low-frequency filter bandwidths were 2 and 10 kHz for the MAS/OMAS and static measurements, respectively. Chemical shifts are reported with respect to an external standard of $Cd(NO_3)_2 \cdot 4H_2O$, and negative shifts are downfield (decreased shielding). Because of the possibility of bulk susceptibility errors,[6] shieldings are believed accurate to ±5 ppm. All measurements were made at room temperature.

Preparation of Samples. Hydrate samples were prepared from reagent-grade $3CdSO_4 \cdot 8H_2O$ crystals (Fisher No. 72089). In fact, quantitative analysis showed this reagent to be 47.0 ± 2% Cd and 15.5 ± 0.1%

† Operated for the U.S. Department of Energy by Iowa State University under Contract No. W-7405-Eng-82. This research was supported by the Assistant Secretary for Energy Research, Office of Energy Sciences, WPAS-KC-03-02-01.

(1) Mehring, M. "High Resolution NMR Spectroscopy in Solids"; Springer-Verlag: Berlin, 1976.
(2) Cheung, T. T. P.; Worthington, L. E.; Murphy, P. DuBois; Gerstein, B. C. *J. Magn. Reson.* **1980**, *41*, 158.
(3) Lipson, H. *Proc. R. Soc. London, Ser. A* **1936**, *156*, 462.
(4) Stejskal, E. O.; Schaefer, J.; McKay, R. A. *J. Magn. Reson.* **1977**, *25*, 569.
(5) Taylor, R. E.; Pembleton, R. G.; Ryan, L. M.; Gerstein, B. C. *J. Chem. Phys.* **1979**, *71*, 4541.
(6) Pople, J. A.; Schneider, W. G.; Berstein, H. J. "High-Resolution Nuclear Magnetic Resonance"; McGraw-Hill: New York, 1959.

0002-7863/81/1503-3282$01.25/0